Acta Oceanol. Sin., 2017, Vol. 36, No. 9, P. 101–107
DOI: 10.1007/s13131-017-1115-y
http://www.hyxb.org.cn
E-mail: hyxbe@263.net

An ocean current inversion accuracy analysis based on a Doppler spectrum model

BAO Qingliu[1, 2*], ZHANG Youguang[1], LIN Mingsen[1], GONG Peng[2]

[1] Key Laboratory of State Oceanic Administration for Space Ocean Remote Sensing and Application, National Satellite Ocean Application Service, State Oceanic Administration, Beijing 100081, China

[2] Key Laboratory of Ministry of Education for Earth System Modeling, Department of Earth System Science, Tsinghua University, Beijing 100084, China

Received 5 April 2016; accepted 13 March 2017

Abstract

Microwave remote sensing is one of the most useful methods for observing the ocean parameters. The Doppler frequency or interferometric phase of the radar echoes can be used for an ocean surface current speed retrieval, which is widely used in spaceborne and airborne radars. While the effect of the ocean currents and waves is interactional. It is impossible to retrieve the ocean surface current speed from Doppler frequency shift directly. In order to study the relationship between the ocean surface current speed and the Doppler frequency shift, a numerical ocean surface Doppler spectrum model is established and validated with a reference. The input parameters of ocean Doppler spectrum include an ocean wave elevation model, a directional distribution function, and wind speed and direction. The suitable ocean wave elevation spectrum and the directional distribution function are selected by comparing the ocean Doppler spectrum in C band with an empirical geophysical model function (CDOP). What is more, the error sensitivities of ocean surface current speed to the wind speed and direction are analyzed. All these simulations are in Ku band. The simulation results show that the ocean surface current speed error is sensitive to the wind speed and direction errors. With VV polarization, the ocean surface current speed error is about 0.15 m/s when the wind speed error is 2 m/s, and the ocean surface current speed error is smaller than 0.3 m/s when the wind direction error is within 20° in the cross wind direction.

Key words: Doppler spectrum model, ocean surface current speed, parameter sensitivity analysis, measurement error

Citation: Bao Qingliu, Zhang Youguang, Lin Mingsen, Gong Peng. 2017. An ocean current inversion accuracy analysis based on a Doppler spectrum model. Acta Oceanologica Sinica, 36(9): 101–107, doi: 10.1007/s13131-017-1115-y

1 Introduction

The ocean current is one of the most important ocean dynamics parameters. It is closely related to the human activity. The mesoscale activity represents over 98% of the ocean's kinetic energy content and has direct implications for the mixing of water masses and the transport of water properties (Baynes et al., 2002). The term mesoscale usually refers to oceanic features between 50 and 200 km, which propagate slowly and can persist for several days to several months. Improved measurements of the mesoscale activity are important to better understand the role of these processes on a global scale and for the verification of ocean models. Microwave remote sensing is one of the most useful methods for the ocean surface current measurement. For example, an along-track interferometry synthetic aperture radar (SAR) (Romeiser et al., 2010) and Doppler scatterometer (Bao et al., 2015) are two sensors for the ocean surface current speed observation. While, the Doppler frequency shifts of the radar echoes are not only determined by the ocean surface current. They also contain the contribution of the ocean wave's motion. The interaction between the ocean current and wave make it difficult for a current speed inversion.

In the past decades, some researchers have established several Doppler spectrum models to elaborate a wave-current interaction. For example, Thompson (1989) proposed the time- dependent composite model of Doppler spectrum in 1989. This model is based on Maxwell Equation, the computational efficiency is much lower. In 2000, Romeiser and Thompson (2000) established a numerical ocean surface Doppler spectrum model for Along-Track interferometric radar imaging. This model was based on Bragg scattering theory in a composite surface model approach. The computation time of this model was reduced by more than one order of magnitude. Fois et al. (2015) established an analytical model of the full-polarimetric sea surface Doppler signature in 2015. This model was based on the second-order small-slop-approximation (SSA) theory and considered the nonlinear properties of the sea surface. All these models described the Doppler properties of the ocean surface. In this paper, we use the numerical ocean surface Doppler spectrum model established by Romeiser and Thompson (2000) to analyze the parameter sensitivity.

The theory of the Doppler spectrum model is shown in Section 2. Section 3 compares the Doppler spectrum model with an

Foundation item: The National Natural Science Foundation of China under contract No. 41606202; the National Key Research and Development Program of China under contract No. 2016YFC1401002; the Open Fund of Key Laboratory of State Oceanic Administration (SOA) for Space Ocean Remote Sensing and Application under contract No. 201601001.
*Corresponding author, E-mail: baoqingliu2000@163.com

empirical geophysical model function (CDOP). The suitable ocean wave elevation spectrum and directional distribution function are selected. The error sensitivity of the ocean surface current speed to the wind speed and direction are analyzed in Section 4. Finally, the conclusions are given in Section 5.

2 Numerical Doppler spectrum model

In general, the Doppler frequency f_D of a moving target can be expressed as

$$f_D = -k_e v_r/\pi, \tag{1}$$

where k_e is the magnitude of the electromagnetic wave vector and v_r is the line-of-sight speed component of the target. In our convention, a positive value of the line-of-sight speed component of the target, thus a negative Doppler frequency, corresponds to a target which is receding from the radar.

For moderate incidence angles, the backscattering of microwaves on the ocean surface is dominated by resonant Bragg scattering. Thus, some doppler shift will always result from the phase speed of the Bragg waves on the ocean surface. If there are no surface currents and long waves, the Doppler spectrum would be two lines with plus and minus frequency, corresponding to the speed of the Bragg wave components traveling toward and away from the radar. The magnitude of the two lines would be proportional to the wave height spectral densities of the Bragg wave components. If there are surface currents, both lines would experience an additional frequency shift in the same direction. And the two lines of the Doppler spectrum will be broadened due to the presence of orbital motions of the long waves.

2.1 *Doppler spectrum*

Doppler spectrum can be considered as the distribution of Doppler frequencies associated with standardized small elements of a backscattered power. Assuming that a single sinusoidal exists, we can get the first moments of the Doppler spectrum (Romeiser and Thompson, 2000):

$$\begin{aligned}\langle f_{D\pm}\rangle_\sigma &= \frac{\langle f_{D\pm}\sigma_\pm\rangle}{\langle\sigma_\pm\rangle}\\ &= \frac{1}{2\pi}\int_0^{2\pi}\left(f_{D\pm}^{(0)} + \mathrm{Re}\left\{Dk\zeta e^{-i\alpha}\right\}\right)\times\\ &\quad\left(1+\mathrm{Re}\left\{M_{1\pm}k\zeta e^{-i\alpha}+M_{2\pm}k^2\zeta^2 e^{-i2\alpha}\right\}\right)\mathrm{d}\alpha\\ &= f_{D\pm}^{(0)} + \frac{1}{2}\mathrm{Re}\left\{D^* M_{1\pm}\right\}k^2\zeta^*\zeta\,,\end{aligned} \tag{2}$$

where D is the complex Doppler modulation transfer function (MTF); k is the wavenumber; $M_{1\pm}$ is a liner MTF describing the relation between first-order slop and NRCS oscillations; ζ is the surface elevation; $\alpha = \vec{k}\cdot\vec{x} - \omega t$; $\langle f_{D\pm}\rangle_\sigma$ is the expectation value of the normalized radar cross-section (NRCS) weighted Doppler frequency; and $f_{D\pm}^{(0)}$ denotes the zeroth-order Doppler frequency. When there are no ocean surface current, the zeroth-order Doppler frequency is the Doppler frequency due to the Bragg wave phase speed, and written as

$$f_{D\pm}^{(0)} = \mp\frac{1}{2\pi}\left\{gk_B\left[1+\left(\frac{k_B}{k_0}\right)^2\right]\right\}^{0.5}, \tag{3}$$

where g is the gravitational acceleration; k_0=363 rad/m. If the ocean surface current exists, the zeroth-order Doppler frequency can be written as the sum of Doppler frequencies caused by the Bragg wave phase speed and the ocean surface current speed (Thompson, 1989; Thompson et al., 1991):

$$f_{D\pm}^{(0)} = \mp\frac{1}{2\pi}\left\{gk_B\left[1+\left(\frac{k_B}{k_0}\right)^2\right]\right\}^{0.5} + \frac{1}{2\pi}\vec{k}_B\cdot\vec{V}\,, \tag{4}$$

where $\vec{k}_B$ is the vector of Bragg wavenumber, and $\vec{V}$ is the vector of the ocean surface current speed.

Similarly, the secondary moment of the Doppler spectrum can be expressed as

$$\begin{aligned}\left\langle f_{D\pm}^2\right\rangle_\sigma &= \frac{\left\langle f_{D\pm}^2\sigma_\pm\right\rangle}{\langle\sigma_\pm\rangle}\\ &= \frac{1}{2\pi}\int_0^{2\pi}\left(f_{D\pm}^{(0)} + \mathrm{Re}\left\{Dk\zeta e^{-i\alpha}\right\}\right)^2\times\\ &\quad\left(1+\mathrm{Re}\left\{M_{1\pm}k\zeta e^{-i\alpha}+M_{2\pm}k^2\zeta^2 e^{-i2\alpha}\right\}\right)\mathrm{d}\alpha\\ &= \left(f_{D\pm}^{(0)}\right)^2 + f_{D\pm}^{(0)}\,\mathrm{Re}\left\{D^* M_{1\pm}\right\}k^2\zeta^*\zeta +\\ &\quad\frac{1}{2}D^* Dk^2\zeta^*\zeta + O(\zeta^4)\,.\end{aligned} \tag{5}$$

Ignore the higher-order terms (higher than the second-order term), using Eqs (2) and (5) we can calculate the variance of sinusoid wave with ζ as its magnitude

$$\left\langle f_{D\pm}^2\right\rangle_\sigma - \langle f_{D\pm}\rangle_\sigma^{\,2} = \frac{1}{2}D^* Dk^2\zeta^*\zeta\,. \tag{6}$$

Now, take the whole wave spectra into account. The real ocean waves consist of a series of sinusoid waves with different frequencies, different magnitudes, different phases, different directions and independent with each other. Thus, the mean and variance of ocean Doppler frequency of the wave spectra can be expressed as the integration of that of single sinusoid wave (Romeiser and Thompson, 2000):

$$\begin{aligned}\langle f_{D\pm}\rangle_\sigma = f_{D\pm}^{(0)} +\\ \mathrm{Re}\left\{\iint D^*(\vec{k})M_{1\pm}(\vec{k})k^2\psi(\vec{k})\mathrm{d}^2k\right\}\,,\end{aligned} \tag{7}$$

$$\begin{aligned}\gamma_{D\pm}^2 = \left\langle f_{D\pm}^2\right\rangle_\sigma - \langle f_{D\pm}\rangle_\sigma^{\,2} =\\ \iint D^*(\vec{k})D(\vec{k})k^2\psi(\vec{k})\mathrm{d}^2k\,,\end{aligned} \tag{8}$$

where ψ denotes the wave height spectrum defined by

$$\psi(\vec{k})\delta(\vec{k}-\vec{k}') = \frac{1}{2}\left\langle\widehat{\zeta}^*(\vec{k}')\widehat{\zeta}(\vec{k})\right\rangle\,. \tag{9}$$

The integrations in Eqs (7) and (8) are all directions and wavenumbers up to 1/6 of the Bragg wave number.

According to the central limit theorem, the distributions of the Doppler frequencies as sums of large numbers of independent contributions must be Gaussian distributions. The mean and variance of Doppler frequencies $f_{D\pm}$ are $\langle f_{D\pm}\rangle_\sigma$ and $\gamma_{D\pm}^2$. Using the mean and variance given by Eqs (7) and (8), and normalizing the Doppler frequencies by the NRCS, we can get a probability density function:

$$S(f_{\mathrm{D}}) = \frac{\langle \sigma_{+} \rangle}{\sqrt{2\pi\gamma_{\mathrm{D}+}^2}} \mathrm{e}^{-(f_{\mathrm{D}}-\langle f_{\mathrm{D}+} \rangle_{\sigma})^2/\gamma_{\mathrm{D}+}^2} + \frac{\langle \sigma_{-} \rangle}{\sqrt{2\pi\gamma_{\mathrm{D}-}^2}} \mathrm{e}^{-(f_{\mathrm{D}}-\langle f_{\mathrm{D}-} \rangle_{\sigma})^2/\gamma_{\mathrm{D}-}^2} , \quad (10)$$

2.2 *Doppler spectrum model validation*

Thompson (1989) proposed the time-dependent composite model of Doppler spectra from the ocean surface. This model is based on fundamental electrodynamic expressions, and the availability of this model is validated by comparing it with the observation results in L band and Ku band.

In order to validate the numerical model of this paper, we compare it with the time-dependent composite model, and the results are shown in Fig. 1. Figure 1 shows the simulation results of the ocean Doppler spectra for L band (1.0 GHz), VV polarization, an incidence angle of 30°, a radar look direction of 75° with respect to the downwind direction, and wind speed of 3 m/s. From Fig. 1, we can know that the results of the numerical Doppler spectrum model are consistent with those of time-dependent composite model.

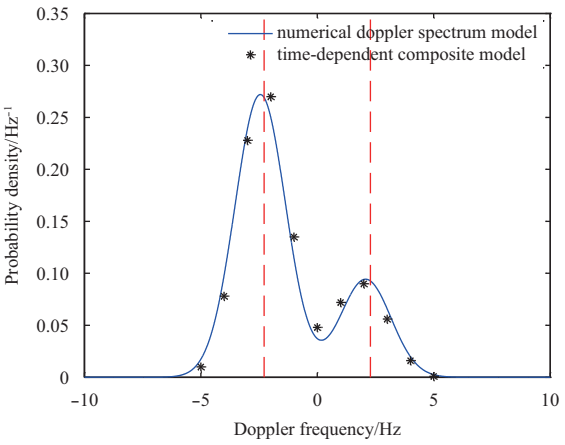

Fig. 1. The validation of the numerical Doppler spectrum model.

3 Selection of input parameters by comparing with CDOP model

3.1 *CDOP model introduction*

The CDOP model is an empirical geophysical model function in C band that used to predict Doppler shifts at both VV and HH polarization as function of the wind speed, the radar incidence angle, and the wind direction with respect to the radar look direction. Thus the CDOP model (Mouche et al., 2008, 2012) can be expressed as

$$f_{\mathrm{D}} = f_{\mathrm{CDOP}}(\phi, u_{10}, \theta, pol) , \quad (11)$$

where f_{D} represents the Doppler frequency anomaly; ϕ is the wind direction with respect to radar look direction; u_{10} is the wind speed at 10 m height; θ is the incident angle; and *pol* is for VV or HH.

The CDOP model is derived from the Doppler centroid anomaly of Envisat ASAR. A match-up database between the wind speed and direction from European Centre For Medium Range Weather Forecasts (ECMWF), collocated with the incidence angle and Doppler measurements from the ASAR is established. There are 277 211 and 350 007 co-locations for VV and HH polarizations, respectively. For HH the RMS and mean difference between the CDOP model and measured Doppler are 6.5 and 1.8 Hz, respectively. For VV the RMS and the mean difference were found to be 5.23 and 1.58 Hz, respectively. The detail of CDOP model is described in the paper of Mouche et al. (2012).

3.2 *Selection of directional distribution functions*

There are two types of the directional distribution function that have been widely used: Cosine-shape and Gaussian-shape. The Cosine-shape directional distribution function (Longuet-Higgins et al., 1963) can be expressed as

$$D(k,\varphi) = \cos\left(\frac{\varphi - \varphi_w}{2}\right)^{2s} , \quad (12)$$

where the spreading parameter (Mitsuyasu et al., 1975) is, in general, a function of wave number k, and the wind speed U_{10}. It can be written as

$$s = 11.5(c/U_{10})^{2.5} \qquad k > k_{\mathrm{p}} . \quad (13)$$

The Gaussian-shape directional distribution function (Apel, 1994) can be expressed as

$$D(k,\varphi) = \exp\left[\frac{-(\varphi - \varphi_w)^2}{2\phi_s^2(k)}\right] , \quad (14)$$

where ϕ_s can be written as

$$\phi_s = \left[0.28 + 10\left(\frac{k}{k_{\mathrm{p}}}\right)^{-1.3}\right]^{-0.5} . \quad (15)$$

The comparison of two types of the directional distribution functions is given in Fig. 2. The spreading parameter of the Cosine-shape function (star dotted curve) is s=2, and the wave number of the Gaussian-shape function (solid curve) ranges from 0.1 to 500.0 rad/s. From Fig. 2, we can see that the Gaussian-shape function broaden and the difference between upwind and downwind increases with the increase of wavenumber. What is more, the upwind and downwind difference of the Cosine-shape function is bigger than that of the Cosine-shape function.

In this section, we simulate the Doppler frequency shift of the Cosine-shape and Gaussian-shape directional distribution functions with different observation azimuths in C band. Then the simulated Doppler frequency shifts were normalized and compared with the CDOP model. The results are shown in Fig. 3.

From Fig. 3, we can see that normalized Doppler frequency shift of the Cosine-shape directional distribution function fits the CDOP model better than that of Gaussian-shape. But for VV polarization, the up/down wind difference of the CDOP model is greater than that of the simulated Doppler frequency shift for both Cosine-shape and Gaussian-shape directional distribution functions. For HH polarization, the normalized Doppler frequency shift of the Cosine-shape directional distribution function fits very well with the CDOP model. Thus, we choose the Cosine-shape directional distribution function as the input parameter of the numerical Doppler spectrum model introduced in Section 2.

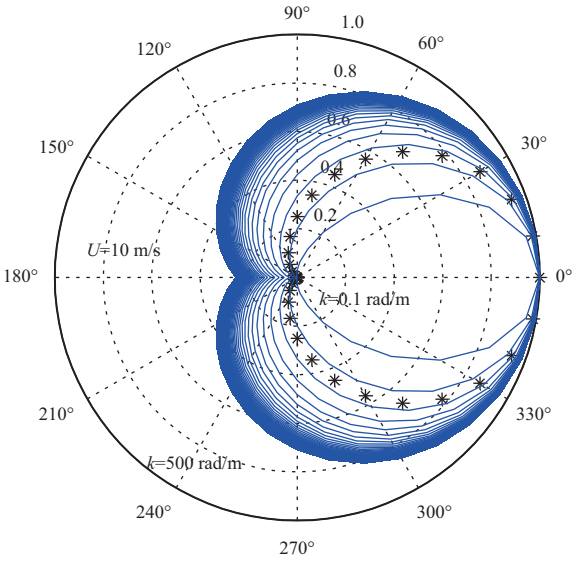

Fig. 2. Comparison of Cosine-shape and Gaussian-shape directional distribution functions.

3.3 *Selection of ocean wave spectrum models*

Bjerkaas-Riedel (1979) spectrum, Elfouhaily et al. (1997) spectrum, and Apel (1994) spectrum are three typical ocean wave models and have been widely used in the literature and simulation models. While different ocean wave spectra have different characteristics and applications. The ocean wave spectra are different with each other even in the same wind speed condition. Figure 4 compares the wave slop spectrum and wave curvature spectrum of the three typical ocean wave models in moderate wind speed condition.

Figure 4 shows that the wave slop spectrum, and wave curvature spectrum of the three typical ocean wave models are different with each other significantly, especially in the vicinity of wavenumber 100–200 rad/s. Meanwhile, ocean waves in this range are dominated for Ku band Bragg scattering. From Eqs (7) and (8) we can know that the mean and variance of the Doppler spectrum are calculated by the integral of the ocean wave slop spectrum. Thus, the selection of the ocean wave model affects the Doppler spectrum directly.

Different ocean wave spectrum models have different performances, as shown in Fig. 4. In this section, the Doppler frequency shifts of three typical ocean wave models with the wind speed in the upwind direction are simulated and compared with the CDOP model. The results are given in Fig. 5. The CDOP model is plotted in the method of error bar. From Fig. 5 we can see that the Doppler frequency shifts of Bjerkaas-Riedel and Elfouhaily et al. spectra are much higher than the CDOP model. The Doppler frequency shifts of Apel spectrum is close to the CDOP model, except for the HH polarization and at high wind speed. Comparing with the CDOP model, the simulated Doppler frequency shift difference is smaller than 10 Hz for VV polarization.

3.4 *Comparison with CDOP model*

We simulate the Doppler frequency shift versus the azimuth angle for both VV and HH polarizations in C band, using Cosine-

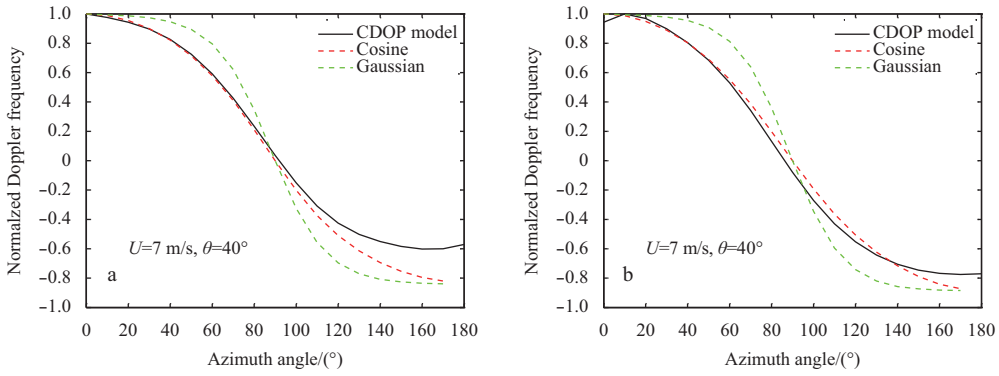

Fig. 3. The normalized Doppler frequency shift of the different directional distribution functions. a. VV polarization, and b. HH polarization.

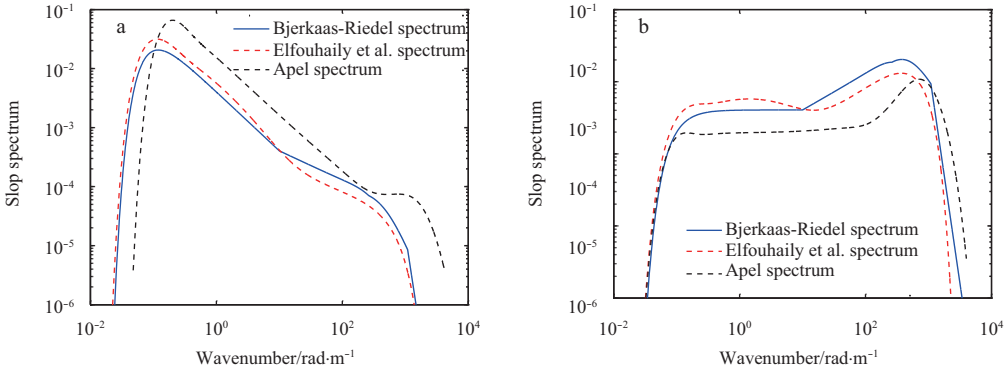

Fig. 4. Comparison of the three typical ocean wave models (U=10 m/s). a. wave slop spectrum, and b. wave curvature spectrum.

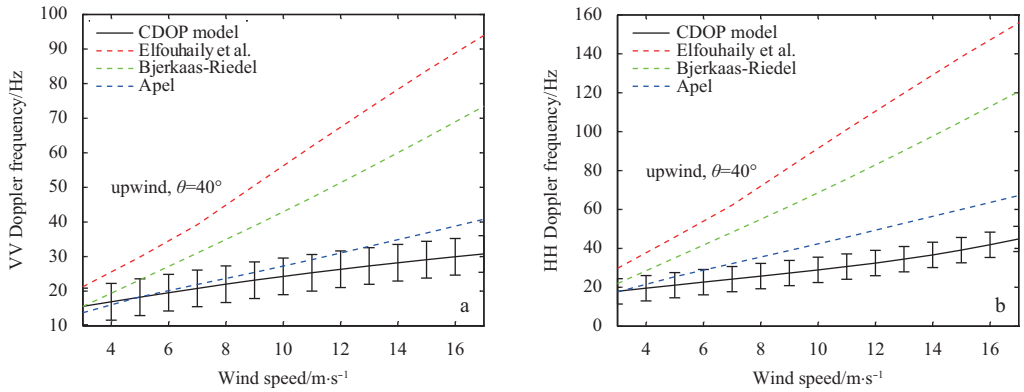

Fig. 5. Doppler frequency shifts of different ocean wave spectrum models in upwind direction. a. VV polarization, and b. HH polarization.

shape directional distribution function and Apel spectrum as the ocean wave model. The wind speed is 6 m/s and the incident angle is 40°. The comparison of the simulated Doppler frequency shift with the CDOP model is shown in Fig. 6. The CDOP model is plotted in the method of error bar. Figure 6 shows that the simulated Doppler frequency shift is basically consistent with the CDOP model. At upwind and downwind directions the simulated Doppler frequency shift is little bigger than the CDOP model, but still within the RMS of the CDOP model. For HH polarization, the Doppler frequency shift differences in upwind and downwind directions are smaller than 7 Hz.

4 Sensitivity analyses of input parameters

The input parameters of the ocean surface Doppler spectrum model include wind speed and wind direction. A local wind field vector can be obtained from the real time measurement by the scatterometer or global wind field forecast by the ECMWF. But both the real time measurement and numerical forecasting are not sufficient accurate. The error of input parameters of Doppler spectrum model will transfer to the simulation results. Thus, in order to inverse the ocean surface current speed using the forward Doppler spectrum model, we need to analyze the sensitivity of the Doppler spectrum model to the input parameters. In this section, the sensitivity analyses of the wind speed and the wind direction are simulated.

4.1 *Sensitivity analyses of wind speed*

There are currently three scatterometers in orbit: HY-2A scatterometer, ASCAT, and RapidScat, which can offer the near real time wind speed and wind direction data. Meanwhile, measurement errors exist as well. For example, the design specification of HY-2A scatterometer is that the RMS of the wind speed should be smaller than 2 m/s. The error of the wind speed will lead to the estimation error of the ocean surface current.

In this section, we use the Cosine-shape directional distribution function and the Apel spectrum as the ocean wave model in the simulations. The ocean current speed estimation errors at different wind speeds in upwind and downwind directions are simulated. The simulation results are shown in Figs 7 and 8. From Fig. 7 we can see that the HH polarization is more sensitive to the wind speed error than the VV polarization in the ocean surface current speed inversion. For the VV polarization, in order to make sure that the ocean surface current speed error is smaller than 0.1 m/s, the wind speed measurement error must be smaller than 1.5 m/s. While, for the HH polarization, if we want to get the same ocean surface current speed accuracy as the VV polarization, the wind speed measurement error must be smaller than 0.8 m/s. Meanwhile, by comparing Figs 7 and 8, we can find that the ocean current speed error in the upwind direction is more sensitive to the wind speed error than that in the downwind direction. Two meters per second wind speed measurement error will lead to 0.28 m/s ocean surface current speed estimation error in the upwind direction for the HH polarization.

4.2 *Sensitivity analyses of wind direction*

Like the wind speed, the wind direction also has a measurement error. For example, the specification of HY-2 scatterometer is that the RMS of the wind direction measurement should be smaller than 20°. The uncertainty of the wind direction will also lead to the ocean surface current speed estimation error. We also

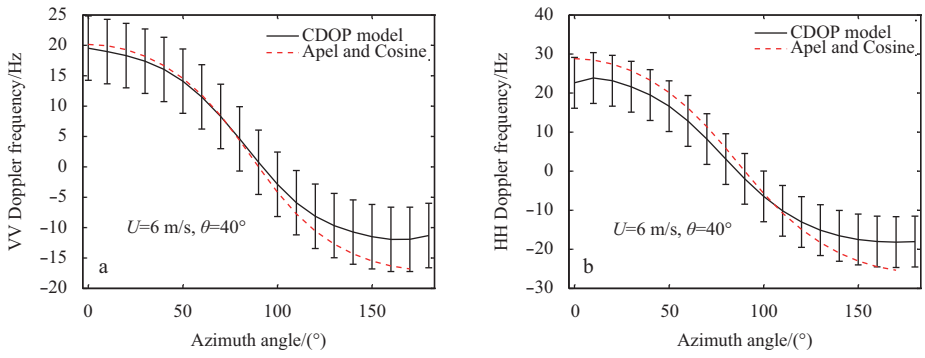

Fig. 6. Comparison of simulated doppler frequency shift with CDOP model. a. VV polarization and, b. HH polarization.

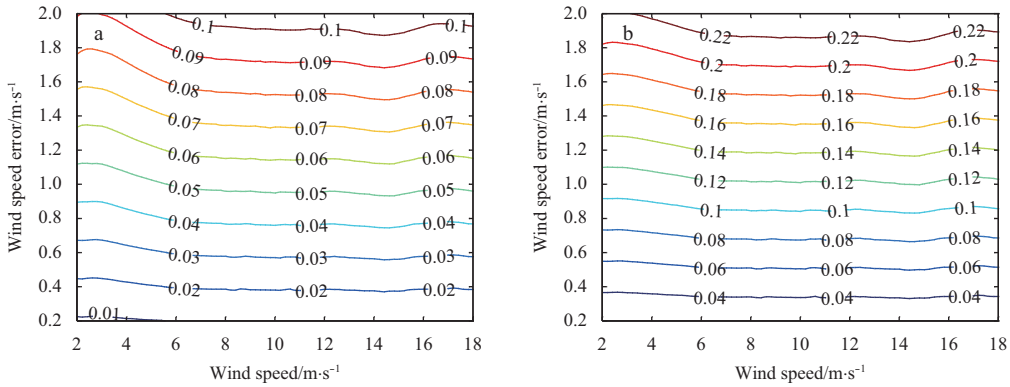

Fig. 7. Ocean current speed estimation errors due to wind speed errors in downwind direction. a. VV polarization, and b. HH polarization.

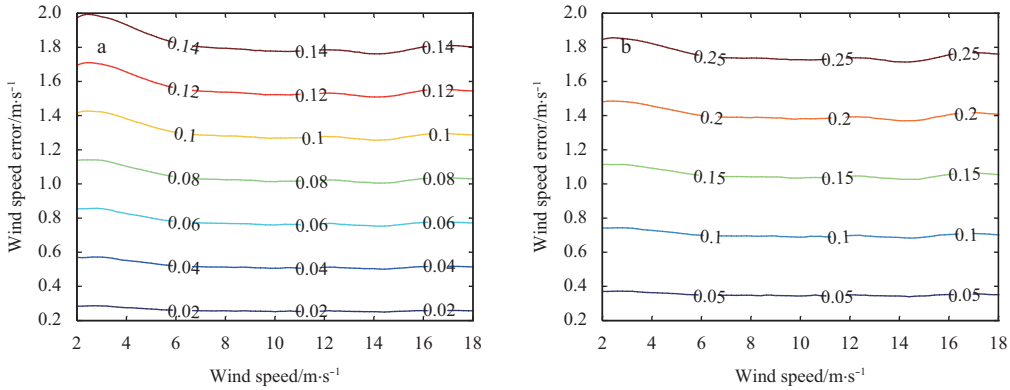

Fig. 8. Ocean current speed estimation errors due to wind speed error in upwind direction. a. VV polarization, and b. HH polarization.

use the Cosine-shape directional distribution function and Apel spectrum as the ocean wave model in the simulation, and the wind speed is set to 7 m/s. The ocean surface current speed estimation errors caused by the wind direction errors for VV and HH polarizations are shown in Figs 9a and b, respectively. From Fig. 9 we can see that the ocean surface current speed estimation error is not sensitive to the wind direction error in the upwind and downwind directions, but it is very sensitive to the wind direction error in the crosswind direction. Similarly, by comparing Figs 9a and b, we can find that the ocean surface current speed estimation error is more sensitive to wind direction error for HH polarization than that for VV polarization. 20° wind direction error will lead to 0.3 m/s ocean surface current speed estimation error in crosswind direction for VV polarization.

5 Conclusions

The ocean surface Doppler spectrum is a forward model to describe the relationship between Doppler frequency shift and the wind speed and direction. And it is usually used to retrieve the ocean surface current. The input parameters of ocean surface Doppler spectrum model, wind speed and wind direction, always have measurement errors. In order to understand the inversion accuracy of ocean current, we need to analyze the parameter sensitivity of the Doppler spectrum model first.

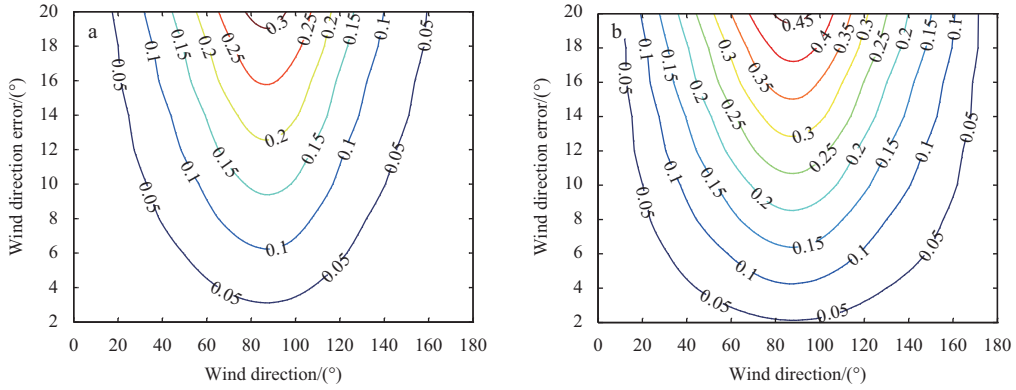

Fig. 9. Ocean current speed estimation error caused by wind direction error. a. VV polarization, and b. HH polarization.

In this paper, we use the numerical ocean surface Doppler spectrum model to analyze its sensitivity to input parameters. Firstly, we simulated the Doppler frequency shift for both VV and HH polarizations in C band. The simulated Doppler frequency shift are compared with the empirical geophysical model function (CDOP model). The simulation results, when using Cosine-shape directional distribution function and Apel spectrum as the ocean wave model, are basically consistent with the CDOP model. Then the sensitivity analyses of wind speed and wind direction are simulated. The results show that the ocean surface current speed estimation error is sensitive to the wind field vector uncertainty. For VV polarization, 2 m/s wind speed measurement error will lead to 0.15 m/s ocean surface current speed estimation error in upwind direction, and 20° wind direction error will lead to 0.3 m/s ocean surface current speed estimation error in crosswind direction. Moreover, the ocean surface current speed estimation error is more sensitive to wind speed and direction error for HH polarization than that for VV polarization. Thus the VV polarization data is better for the ocean surface current speed inversion.

Compared with the wind field, the ocean current is a slow varying ocean parameter. Normally, the temporal resolution of the ocean surface current product for open sea is more than 5 d. The inversion accuracy can be improved by averaging in time domain. For doppler scatterometer, its swathe is larger than 1 000 km and it can coverage more than 85% of the global ocean each day. Thus, the current speed inversion accuracy could be better than 0.15 m/s if the temporal resolution of ocean current product is more than 5 days.

Acknowledgements

The authors wish to thank Mouche Alexis in the IFREMER for the provision of the empirical geophysical model function CDOP and appreciate the helps that he gives.

References

Apel J R. 1994. An improved model of the ocean surface wave vector spectrum and its effects on radar backscatter. Journal of Geophysical Research, 99(C8): 16269–16291

Bao Qingliu, Dong Xiaolong, Zhu Di, et al. 2015. The feasibility of ocean surface current measurement using pencil-beam rotating scatterometer. IEEE Journal of Selected Topics in Applied Earth Observations and Remote Sensing, 8(7): 3441–3451

Baynes P, Dumper K, Gommenginger C, et al. 2002. Ocean currents from space. BNSC SMS Programme, Document No: SOS-OC-REP-2/01

Bjerkaas A W, Riedel F W. 1979. Proposed model for the elevation spectrum of a wind-roughened sea surface. DTIC Document No: JHU/APL TG 1328

Elfouhaily T, Chapron B, Katsaros K, et al. 1997. A unified directional spectrum for long and short wind-driven waves. Journal of Geophysical Research, 102(C7): 15781–15796

Fois F, Hoogeboom P, Chevalier F L, et al. 2015. An analytical model for the description of the full-polarimetric sea surface Doppler signature. Journal of Geophysical Research, 120(2): 988–1015

Longuet-Higgins M S, Cartwright D E, Smith N D. 1963. Observations of the directional spectrum of sea waves using the motions of a floating buoy. In: Ocean Wave Spectrum. Englewood Cliffs, NJ: Prentice-Hall Inc, 111–136

Mitsuyasu H, Tasai F, Suhara T, et al. 1975. Observations of the directional spectrum of ocean waves using a cloverleaf buoy. Journal of Physical Oceanography, 5(4): 750–760

Mouche A A, Chapron B, Reul N, et al. 2008. Predicted Doppler shifts induced by ocean surface wave displacements using asymptotic electromagnetic wave scattering theories. Waves in Random and Complex Media, 18(1): 185–196

Mouche A A, Collard F, Chapron B, et al. 2012. On the use of Doppler shift for sea surface wind retrieval from SAR. IEEE Transactions on Geoscience and Remote Sensing, 50(7): 2901–2909

Romeiser R, Johannessen J, Chapron B, et al. 2010. Direct surface current field imaging from space by along-track InSAR and conventional SAR. In: Barale V, Gower J F R, Alberotanza L, eds. Oceanography from Space. Berlin: Springer Netherlands, 73–91

Romeiser R, Thompson D R. 2000. Numerical study on the along-track interferometric radar imaging mechanism of oceanic surface currents. IEEE Transactions on Geoscience and Remote Sensing, 38(1): 446–458

Thompson D R. 1989. Calculation of microwave Doppler spectra from the ocean surface with a time-dependent composite model. In: Komen G J, Oost W A, eds. Radar scattering from modulated wind waves. Berlin: Springer Netherlands, 27–40

Thompson D R, Gotwols B L, Keller W C. 1991. A comparison of K_u-band Doppler measurements at 20° incidence with predictions from a time-dependent scattering model. Journal of Geophysical Research, 96(C3): 4947–4955